JOURNAL OF MATERIALS SCIENCE 32 (1997) 2215–2218

High temperature compression creep of aluminium nitride after immersion in molten stainless steel

I. MASSON*,‡, J. P. FEIEREISEN*, J. P. MICHEL*, A. MOCELLIN‡
*Laboratoire Métallurgie Physique and Science des Matériaux (CNRS, URA 155) and ‡Laboratoire de Science et Génie des Matériaux Métalliques (CNRS, URA 159), Ecole des Mines de Nancy, Parc de Saurupt, 54042 NANCY Cedex, France

P. BLUMENFELD
IRSID, 57210 Maizieres-Les-Metz France

The effect of immersion in molten steel on subsequent creep behaviour has been investigated in two AlN ceramics. Steady-state creep was not significantly affected but an enhanced initial creep rate was observed, especially when the surface layer had not been removed after immersion. In immersed samples, SEM revealed some open porosity and microcracks near the surface and particles containing steel constituents were found by TEM deep inside samples, in grain-boundary secondary phases.

1. Introduction

Aluminium nitride crystallizes in the wurzite structure (2H). It has a high melting point ($\sim$2673 K), an excellent thermal conductivity ($\sim$200 W m^{-1} K^{-1} at room temperature), a good resistance to molten metals and to oxidation at elevated temperatures. These properties, combined with a good mechanical strength, make AlN an attractive material for use as special refractories for metal processing.

The wetting character and corrosion of AlN by liquid aluminium and gallium was studied by Long and Foster [1] who concluded that dense AlN could safely be used as a crucible for these molten metals, since microstructural investigations proved the absence of corrosion although AlN was wetted by both Al and Ga.

The reactivity of dense AlN with body-centred cubic (b c c) refractory metals (niobium, tantalum, molybdenum and tungsten) was studied up to 2273 K [2]. It was shown that both nitrides and aluminides formed from 1673 K with Nb in vacuum and that nitrides form with Ta above 1873 K. No reaction with Mo or W was observed up to 1973 K at which temperature AlN started to dissociate.

More recently, Labbe and Brandy [3] have studied AlN wetting by liquid copper between 1370 and 1570 K by the sessile drop method. They conclude that wetting is very poor for dense AlN ceramics whatever the sintering additive. The same authors also conducted a corrosion study of hot-pressed AlN, with a porosity varying from 1 to 30%, between 1470 and 1670 K [4]. For dense AlN, the corrosion reaction with liquid Cu started at 1473 K. At porosity larger than 2%, diffusion of Cu along the grain boundaries and capillary penetration was observed at 1673 K.

Wetting of AlN by stainless steels was investigated by Sveshkov and Kalmykov [5]. They stated that AlN could be attacked by chromium-containing steels, while it is not wetted by pure iron and nickel. They also observed that the wettability measured by the sessile drop technique is higher in vacuum than in argon atmosphere.

To our knowledge none of these wetting and corrosion studies was complemented by investigation of mechanical properties of the materials submitted to corrosion tests. It is the purpose of this paper to report on such experiments and briefly discuss their meaning in the light of structural changes that have been observed in samples immersed in liquid metals. Mechanical behaviour of AlN ceramics was studied up to 1923 K under different testing conditions. A review of the literature results can be found in [6]. We report here on creep tests in compression carried out on sintered and hot-pressed AlN (respectively, S-AlN and HP-AlN) at temperatures from 1773 to 1973 K in a neutral atmosphere, after immersion in molten stainless steels. A comparison with the data obtained without immersion is provided.

2. Experimental details

Both S- and HP-AlN used in this work were obtained from ESK (Electro Schmelzwerk Kampten). Sintering aids were used and a chemical analysis using inductively coupled plasma emission spectroscopy revealed the presence of $\sim$2 wt % lanthanum in both materials. This corresponds to a volume fraction of nearly

5% for the oxide. Traces of calcium were also detected. The main secondary phase identified by X-ray diffraction and wavelength dispersive analysis was lanthanum aluminate ($La_2O_3 \cdot 11Al_2O_3$).

Scanning electron microscopy (SEM) was used to characterize the distribution of the second phase and also to measure the average grain size of the ceramics. For the latter, the linear intercept method applied to a population of 200 grains lead to $d = 6.9 \pm 2.4\,\mu m$ for S-AlN and $4.1 \pm 1.8\,\mu m$ for HP-AlN.

Test samples for immersion in molten steel were diamond-cut into discs $5 \times 5 \times d\,mm^3$ ($d \leqslant 130\,mm$ for S-AlN and $d \leqslant 200\,mm$ for HP-AlN, d being the diameter of as-supplied discs). Immersion experiments were done in an induction furnace under argon and argon/hydrogen atmospheres, successively, in order to avoid oxidation of the molten metal. The stainless steel contained 18 wt % Cr, 10 wt % Ni and 2 wt % Mn. Bar-shaped samples, fixed in a magnesia holder, were slowly heated and plunged into the bath to avoid thermal shock. Specimens were maintained for one hour in molten steel.

Two types of compression samples were machined out from immersed materials. (1) $5 \times 5 \times 12\,mm^3$ parallelepipeds, i.e. with the layer deposited during immersion kept on the side surfaces. These samples are denoted 1 S-AlN and 1 HP-AlN. (2) $3 \times 3 \times 8\,mm^3$ bars taken at the centre of immersed materials, called hereafter i S-AlN and i HP-AlN.

Creep tests were performed in a MTS 810 machine equipped with a Centorr furnace. The samples were placed between two SiC plates. Tests were conducted in an argon and helium mixture. The strain was recorded using a Linear Voltage Displacement Transducer (LVDT) gauge and temperature by a W/W–Re thermocouple and a pyrometer pointing at the sample. Crept samples were cooled down under applied load. The applied stress ranged from 150 to 250 MPa. In order to spare matter (for immersed materials), stress jumps were done during the creep tests. The resulting variation of the strain rate, $\dot{\varepsilon}$, was measured after ~ 30 min, a time sufficient for a new apparent steady-state to be reached.

For transmission electron microscopy (TEM) observation, slices approximately 0.5 mm thick and 3 mm diameter were diamond-cut at angles of 0°, 45° or 90° off the compression axis. Thin foils were then made by mechanical polishing and dimpler grinding followed by ion milling. TEM work was done with a Jeol 200 CX electron microscope operating at 200 kV. Energy dispersive analysis (EDS) was performed in a Philips CM 12 operating at 120 kV.

3. Results

3.1. Creep curves

The creep behaviour of HP-AlN, as received, after immersion with the stained layer and after immersion and removal of this layer is detailed in Figs 1 to 4. Durations of creep experiments ranged between 3×10^3 and 4×10^4 s, to be compared with the duration of contact with liquid steel in casting experiments, typically 1 h. At the lower temperature, the $\varepsilon = f(t)$ creep curve exhibits two stages: a first transient of very

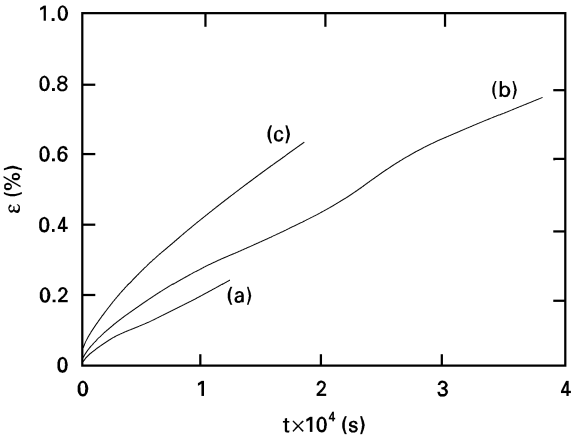

Figure 1 Creep curves (strain versus time) of hot pressed AlN at $\sigma = 250$ MPa, $T = 1773$ K. (a) As-received HP-AlN, (b) i HP-AlN, immersed in molten steel and subsequently crept after removal of the stained surface layer and (c) 1 HP-AlN, immersed in molten steel and subsequently crept without removal of the stained surface layer.

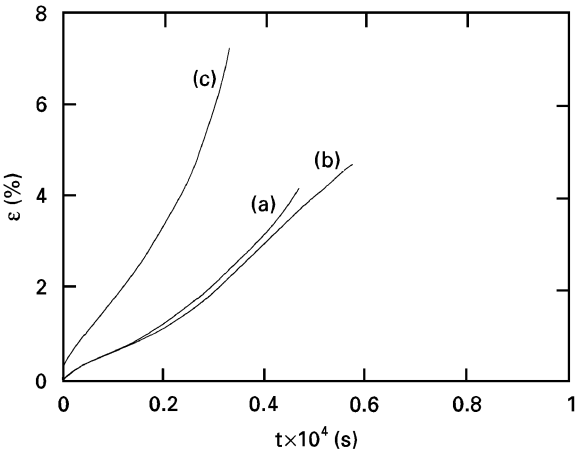

Figure 2 Creep curves (strain versus time) of hot pressed AlN at $\sigma = 250$ MPa, $T = 1973$ K. (a) As-received HP-AlN, (b) i HP-AlN, immersed in molten steel and subsequently crept after removal of the stained surface layer and (c) 1 HP-AlN, immersed in molten steel and subsequently crept without removal of the stained surface layer.

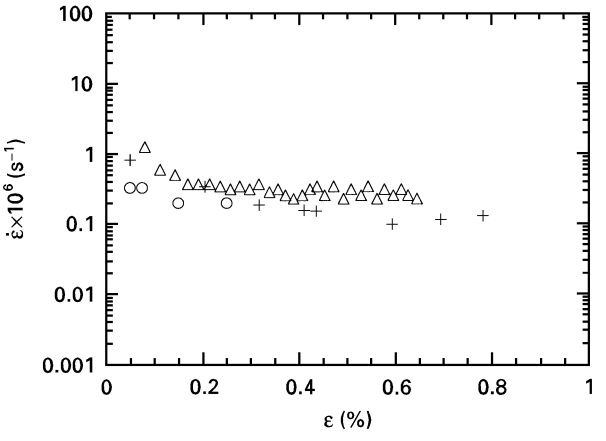

Figure 3 Creep curves (creep strain rate versus creep strain) at $\sigma = 250$ MPa, $T = 1773$ K. (a) As-received HP-AlN (○), (b) i HP-AlN, immersed in molten steel and subsequently crept after removal of the stained surface layer (+) and (c) 1 HP-AlN, immersed in molten steel and subsequently crept without removal of the stained surface layer (Δ).

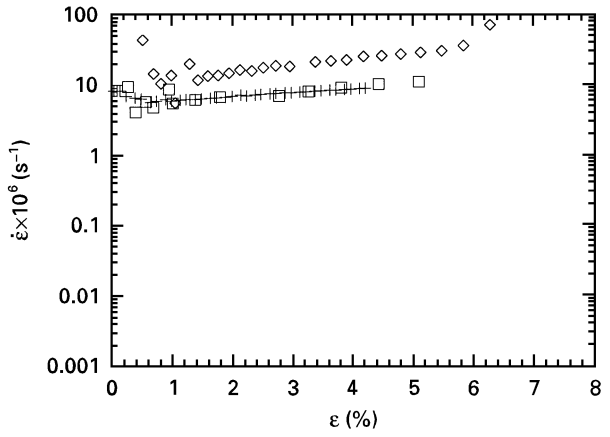

Figure 4 Creep curves (creep strain rate versus creep strain) at $\sigma = 250$ MPa, $T = 1923$ K. (a) As-received HP-AlN (+), (b) i HP-AlN, immersed in molten steel and subsequently crept after removal of the stained surface layer (□) and (c) 1 HP-AlN, immersed in molten steel and subsequently crept without removal of the stained surface layer (◇) .

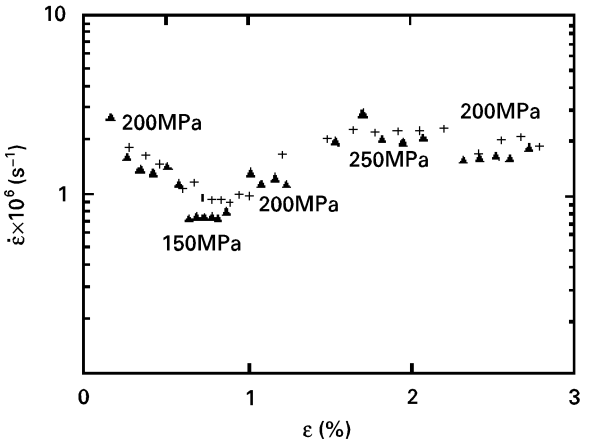

Figure 5 Creep curves (strain rate versus strain) of i S-AlN (▲) and i HP-AlN (+) at 1873 K, with stress jumps.

small duration (10^2 s) is followed by a fairly linear stage, corresponding to some steady-state. At 1923 K, the creep rate is increased by more than one order of magnitude and it is not certain that a steady state has been approached. In Fig. 1, the total creep strain is slightly larger after immersion, though the steady-state creep rate is the same as in as-received AlN, when the surface layer has been removed. With this layer on, creep is faster by 50%. At 1923 K, Fig. 2, no significant difference appears between curves A and B, i.e. as-received material and after immersion and removal of the stained layer. Creep is, however, twice as fast with the stained layer kept on the sample surface.

As seen on Figs 3 and 4, which display the same results or a $\dot{\varepsilon}$ (ε) plot to show the strain dependence of the creep rate, minimum creep rates at $\sigma = 250$ MPa range from $10^{-7}\,s^{-1}$ at 1773 K and $5\times10^{-6}\,s^{-1}$ at 1923 K in as-received material to $2\times10^{-7}\,s^{-1}$ at 1773 K and $10^{-5}\,s^{-1}$ at 1923 K after immersion in molten steel.

Fig. 5 allows comparison of S- and HP-AlN and determination of the stress dependence of creep at 1873 K. In this $\dot{\varepsilon}$ (ε) plot, the creep rate is consistently slightly larger in HP-AlN after immersion and surface layer removal. This is the same behaviour as observed in as-received AlN. It is also shown that stress jumps lead to consistent results, and do not depend much on the previous history of the sample. Indeed, about, the same steady-state creep rate is obtained at a given stress, before and after up and down stress jumps.

Steady-state creep rate, $\dot{\varepsilon}_{ss}$, as a function of stress was plotted for each material and temperature on a log–log scale. The data could be fitted to straight lines, their slopes defining the stress exponent, n. For both i S-AlN and i HP-AlN the average value of n was 1.8 at 1823 and 1873 K.

Similarly, an Arrhénius plot of $\ln\dot{\varepsilon}_{ss}$ versus $1/T$ at constant stress yielded apparent activation energies, Q, equal to 680 and 665 kJ mol^{-1} for i S-AlN and i HP-AlN, respectively, at $\sigma = 250$ MPa. The difference between these two activation energies is not significant. n and Q values appear to be the same as for creep of as-received AlN.

3.2. Microstructural observations

In the as-received state, both S- and HP-AlN show second phase particles located at triple junctions between grains or at some places along grain boundaries. No cavities were observed.

After one hour immersion in molten stainless steel, the samples did not show macroscopic evidence of corrosion or dissolution. A 30 μm thick oxide layer was observed at the surfaces. X-ray qualitative analysis, points to the presence in this layer of all of the metallic constituents of steel: iron, nickel and chromium. No trace of aluminium or lanthanum could be detected inside the layer. The layer was poorly adherant to AlN and was easily removed (Fig. 6).

SEM observations in AlN near the surface also provided evidence of some cavities at grain boundaries and triple points together with microcracks, revealing that some open porosity was produced by dissolution in the melt (Fig. 6). It is also possible that the microcracks form from thermal shock.

TEM observation of thin foils taken from the centre of immersed bars did not show any evolution of grain size and shape. No cavities were detected at any place, at such depths. However, EDS analysis revealed large particles, 2–3 μm in diameter, located in contact with sintering second phases, i.e. at grain boundaries, and containing all steel constituents: iron, nickel, chromium and manganese (Fig. 7). The density was about one particle in 500 μm^2.

The dislocation density was the same as that for as-received materials.

TEM observations were also done in samples immersed and then crept at $\sigma = 250$ MPa, at 1773 and 1923 K. Very clearly, no significant difference in microstructures was seen compared to those obtained by creep under similar conditions, without previous immersion in liquid steel. The grain size and shape were not affected. The density and size of cavities appearing along grain boundaries and at triple points were slightly larger 1.4 μm average diameter and a

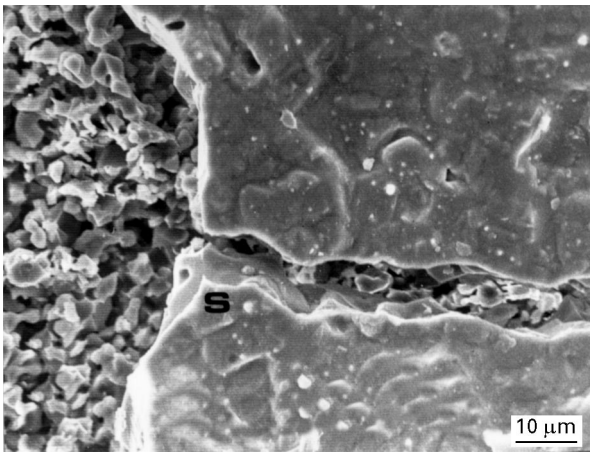

Figure 6 SEM micrograph of HP-AlN bars immersed one hour in molten steel at 1773 K showing a thin layer of steel oxides (S) partly adhesive to the AlN surface and microcracks and open porosity at grain boundaries.

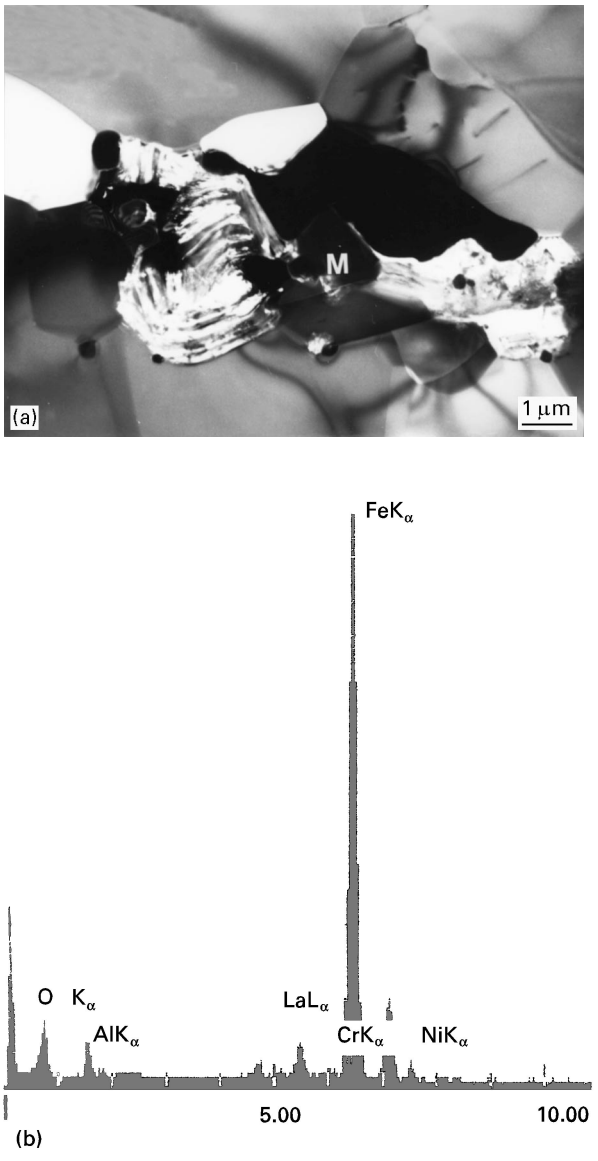

Figure 7 (a) TEM micrograph of a dark metallic particle (M) detected in HP-AlN immersed one hour in molten steel, with (b) EDS analysis.

volume fraction of cavity of 5% in S-AlN after immersion and crept at $\sigma = 250$ MPa, $T = 1923$ K, $\varepsilon = 6.6\%$, instead of 1.0 μm diameter and 3% volume fraction in S-AlN after creep under the same conditions but $\varepsilon = 3.9\%$. The increase of the total strain is believed to be the main cause of enhanced cavitation.

The dislocation density was increased by deformation and most of the dislocations seem to result from limited intragranular plastic deformation, necessary to accommodate the plastic incompatibilities which arose from grain boundary gliding. No evidence was found that the steel particles mentioned above played a part in creep.

4. Summary and conclusions

Creep curves and deformation microstructures made after immersion in molten stainless steel confirm that AlN is very resistant to corrosion by liquid and would be a very good refractory material for steel casting (except that its cost is probably too high).

Immersion for 1 h in liquid steel has only a very minor effect on creep resistance, with an increase in the initial creep rate, when the spongy layer is not removed but with identical steady-state behaviour. As observed in liquid copper, grain boundaries and especially second phases resulting from sintering additives are weaker paths of penetration of the liquid metal in AlN ceramics. Limited dissolution of AlN itself seems, however, to have taken place near the surface.

More surprising was the presence of "steel" particles deep inside the immersed bars. This could be a strong indication that second phases are more or less viscous at the temperature of the steel melt and that these second phases are continuous along grain boundaries and not only confined at isolated triple points. These indications have a validity limited to ESK materials and probably cannot be generalized to all AlN ceramics.

References

1. G. LONG and L. M. FOSTER, *J. Amer. Ceram. Soc.* **42** (1959) 53.
2. A. L. BORISOVA and I. S. MARTSENYUK, *Porosh. Metall.* **154** (1975) 51. (Translation: *Sov. Powder Metall. Met. Ceram.* **14** (1976) 822).
3. J. C. LABBE and G. BRANDY, *Rev. Int. Hautes Tempér. Refract.* **26** (1990) 121.
4. *Idem*, *ibid.* **27** (1991) 69.
5. Y. V. SVESHKOV and V. A. KALMYKOV, *Russ. Metall.* **3** (1973) 37.
6. I. MASSON, J. P. FEIEREISEN, J. P. MICHEL, A. GEORGE, A. MOCELLIN and P. BLUMENFELD, *J. Eur. Ceram. Soc.* **13** (1994) 355.

Received 17 March 1995
and accepted 23 October 1996